Iron Oxo Complexes

DOI: 10.1002/ange.200802219

# An Inverted and More Oxidizing Isomer of $[Fe^{IV}(O)(tmc)(NCCH_3)]^{2+}$**

*Kallol Ray, Jason England, Adam T. Fiedler, Marlène Martinho, Eckard Münck,* and Lawrence Que, Jr.**

High-valent oxoiron species are often invoked as the oxidants in the catalytic cycles of dioxygen-activating mononuclear nonheme iron enzymes.[1] To date, such iron(IV) intermediates have been characterized for four enzymes, lending strong support for this notion.[2] Within the same time frame, synthetic nonheme complexes containing oxoiron(IV) units have also been described that serve as models for such reactive intermediates.[3] The first crystallographically characterized and most extensively studied member of this family of synthetic oxoiron(IV) complexes is $[Fe^{IV}(O)(tmc)(NCCH_3)](OTf)_2$ (**1**-$NCCH_3$; tmc = 1,4,8,11-tetramethyl-1,4,8,11-tetraazacyclotetradecane).[4] Its structure features a short Fe=O bond (1.646 Å) with an acetonitrile bound *trans* to the oxo atom.[4] The macrocyclic tmc ligand adopts a *trans*-I (*R*,*S*,*R*,*S*) configuration,[5] such that all four methyl groups are oriented in the same direction with respect to the $FeN_4$ plane, and *anti* to the oxo atom. On the other hand, monoanionic X ligands coordinate *syn* to the methyl groups in crystal structures of five-coordinate $[Fe^{II}(tmc)(X)]^+$ complexes.[6] Herein, we report the unexpected preparation of an inverted isomer of **1**-$NCCH_3$ in which the oxo group binds to the site *syn* to the four methyl groups (Scheme 1). The conversion of **1**-$NCCH_3$ to its inverted isomer is effected by treatment with PhIO in the presence of tetrafluroborate, an otherwise inert anion. The switch in binding site of the oxo group engenders changes in the spectroscopic properties of the oxoiron(IV) complex and, more importantly, a significantly enhanced reactivity in hydrogen-atom abstraction and oxo-transfer reactions.

The reaction of $[Fe^{II}(tmc)(OTf)](OTf)$ with solid iodosylbenzene (PhIO) (ca. 5 equiv) in $CH_3CN$ at 25 °C affords in quantitative yield pale green **1**-$NCCH_3$ with $\lambda_{max}$ at 820 nm ($\varepsilon = 400\,M^{-1}cm^{-1}$; Figure 1), as described previously.[4] The near-IR band has been assigned to d–d transitions that arise from the $S = 1$ oxoiron(IV) center.[7] However, in the presence of $NBu_4BF_4$, the reaction produces a different species, yellowish green **2**, with bands at 806 ($\varepsilon = 170\,M^{-1}cm^{-1}$) and 1026 nm ($\varepsilon = 190\,M^{-1}cm^{-1}$; Figure 1), absorption features significantly different from those of **1**-$NCCH_3$. Mössbauer analysis of **2** further underscores its distinct nature from **1**-$NCCH_3$. As shown in Figure 1 inset, the 4.2 K Mössbauer spectrum of **2** ($\Delta E_Q = 0.78\,mm\,s^{-1}$, $\delta = 0.14\,mm\,s^{-1}$) is quite distinct from that obtained for **1**-$NCCH_3$ ($\Delta E_Q = 1.24\,mm\,s^{-1}$

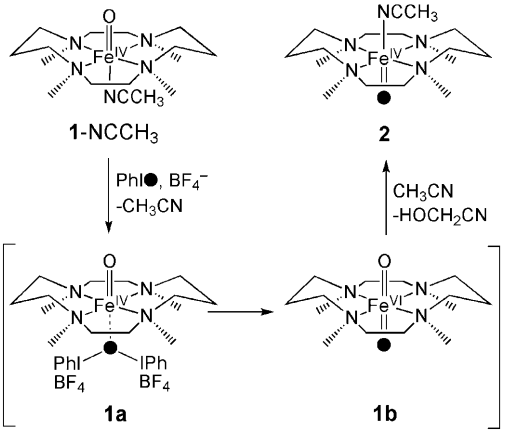


***Scheme 1.*** Mechanism of the conversion of **1**-$NCCH_3$ to **2**.

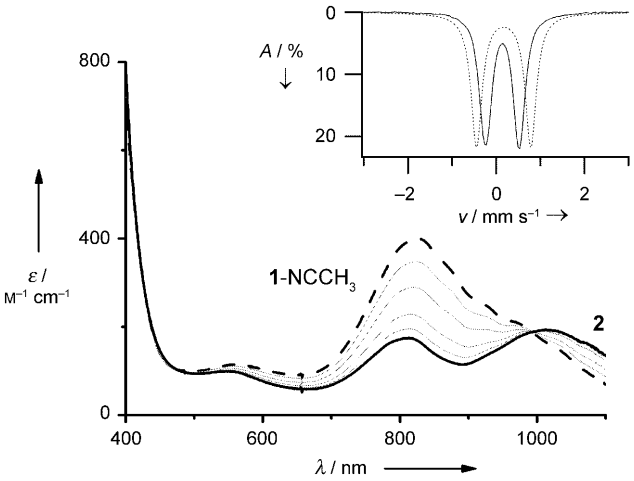


***Figure 1.*** Vis/NIR spectra of **1**-$NCCH_3$ (dashed line) and **2** (dark solid line). Intermediate spectra show the conversion of **1**-$NCCH_3$ to **2** upon successive addition of 1 equiv $PhI(OAc)_2$ in the presence of $NBu_4BF_4$. The inset shows the Mössbauer spectra of **1**-$NCCH_3$ (dashed line) and **2** (solid line) recorded in zero magnetic field at 4.2 K.

[*] Dr. M. Martinho, Prof. Dr. E. Münck
Department of Chemistry, Carnegie Mellon University
Pittsburgh, PA 15213 (USA)
E-mail: emunck@cmu.edu
Dr. K. Ray, Dr. J. England, Dr. A. T. Fiedler, Prof. Dr. L. Que, Jr.
Department of Chemistry and Center for Metals in Biocatalysis
University of Minnesota, Minneapolis, MN 55455 (USA)
Fax: (+1) 612-624-7029
E-mail: larryque@umn.edu

[**] This work was supported by the National Institutes of Health (GM-33162 to L.Q., GM-079839 to A.T.F., and EB-001475 to E.M.). XAS data were collected on beamline 9-3 at the Stanford Synchrotron Radiation Laboratory (SSRL).

Supporting information for this article is available on the WWW under http://dx.doi.org/10.1002/anie.200802219.

and $\delta = 0.17\ mm\,s^{-1}$). However, the zero-field splittings and magnetic hyperfine tensors of **1**-$NCCH_3$ and **2**, determined from studies in strong applied magnetic fields, are practically the same (see Figure S1 and Table S1).

Additional measurements provide further insight into the nature of **2**. Conductivity experiments on **2** in $CH_3CN$ yield an Onsager plot[8] with a slope comparable to those of known 1:2 electrolytes (cation:anion ratio), such as **1**-$NCCH_3$ and $[Fe^{IV}(O)(N4Py)](ClO_4)_2$ (**3**, N4Py = bis(2-pyridylmethyl)-bis(2-pyridyl)methylamine), and much larger than those for known 1:1 electrolytes (e.g. $NBu_4PF_6$ and $NBu_4BF_4$; Figure S2). Therefore **2**, like **1**-$NCCH_3$, is a 1:2 electrolyte. Secondly, electrospray ionization mass spectrometry (ESI-MS) of solutions of isolated **1**-$NCCH_3$ and **2** gives rise to identical spectra, with prominent peaks corresponding to $[Fe(O)(tmc)(NCCH_3)]^{2+}$ ($m/z$ 184.4) and $\{[Fe(O)(tmc)](OTf)\}^+$ ($m/z$ 476.9) ions (Figure S3). Lastly, EXAFS analysis of **2** reveals Fe–ligand distances ($r_{Fe=O} = 1.64$ Å; $r_{Fe-N}(ave) = 2.08$ Å) identical to those found for **1**-$NCCH_3$ (Figure S4 and Table S2). Thus, **1**-$NCCH_3$ and **2** appear to be isomers with the same composition.

How then does **2** differ structurally from **1**-$NCCH_3$? $^1H$ NMR data (Figure 2) limit the possibilities. Since the tmc

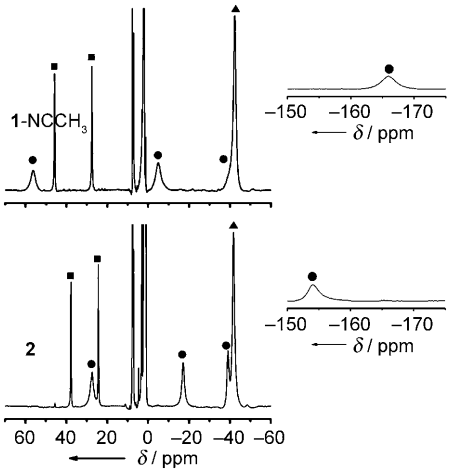


***Figure 2.*** $^1H$ NMR spectra of **1**-$NCCH_3$ and **2** in $CD_3CN$ at 25 °C in the range from 70 to −60 ppm. The insets show the NMR spectra in the range from −150 to −175 ppm. The peaks are assigned to the tmc ligand as follows: ■: $NCH_2CH_2CH_2N$ (2×2 H); ●: $NCH_2$ (4×4 H); ▲: $NCH_3$ (12 H).

ligand in **1**-$NCCH_3$ is known to adopt a *trans*-I configuration,[4] the four methyl groups are equivalent and give rise to a single methyl resonance that is readily assigned by integration. Although distinct from that of **1**-$NCCH_3$, the $^1H$ NMR spectrum of **2** exhibits the high symmetry found in **1**-$NCCH_3$, indicating that the tmc ligand retains a *trans*-I configuration. These results led us inexorably to the conclusion that **2** is simply the inverted isomer of **1**-$NCCH_3$ in which the positions of the oxo and acetonitrile ligands are interchanged (see Scheme 1).

Additional support for the inverted-isomer hypothesis comes from ligand exchange reactions of **1**-$NCCH_3$ and **2** with $NBu_4SCN$. As reported previously,[6a] the reaction between **1**-$NCCH_3$ and $NBu_4SCN$ forms **1**-NCS with a molecular composition of $[Fe(O)(tmc)(NCS)]^+$ as deduced from ESI-MS ($m/z$ 386.1). The analogous reaction with **2** leads to the formation of **2**-NCS with an identical molecular composition by ESI-MS. Although **1**-NCS and **2**-NCS have very similar Mössbauer spectra both in zero and applied magnetic fields (Tables 1 and S1; Figures S5 and S6), their electronic spectra

***Table 1:*** Spectroscopic properties of the complexes.

| Complex | $\lambda_{max}$ [nm] ($\varepsilon$ [$M^{-1}\,cm^{-1}$]) | $\Delta E_Q$ [$mm\,s^{-1}$] | $\delta$ [$mm\,s^{-1}$] |
|---|---|---|---|
| **1**-$NCCH_3$ | 820(400) | 1.24(1) | 0.17(1) |
| **2** | 806(170) | 0.78(2) | 0.14(1) |
| | 1026 (190) | | |
| **1**-NCS | 386 (4200) | 0.60(2) | 0.16(2) |
| | 850 (200) | | |
| | 1010 (160) | | |
| **2**-NCS | 415 (5400) | 0.61(2) | 0.14(1) |
| | 812 (120) | | |
| | 1015 (140) | | |

are clearly distinct, with characteristic absorptions at 386, 850, and 1010 nm for **1**-NCS, and 415, 812, and 1015 nm for **2**-NCS (Figure 3). Additionally, their $^1H$ NMR spectra exhibit different paramagnetic shift patterns (Figure S7). Thus, based on the accumulated data, **1**-NCS and **2**-NCS are best described as position isomers with the positions of the axial oxo and NCS ligands switched.

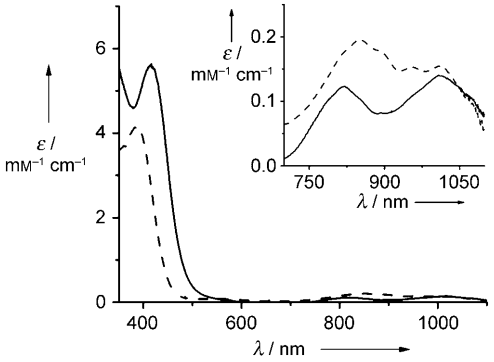


***Figure 3.*** UV/Vis/NIR spectra of **1**-NCS (dashed line) and **2**-NCS (solid line) formed by the reaction of **1**-$NCCH_3$ and **2** with 1 and 5 equiv $NBu_4SCN$, respectively, in $CH_3CN$ at −30 °C. The inset shows the vertical expansion of the NIR region. The extinction coefficients are estimated based on the iron(IV) fractions determined by Mössbauer spectroscopy (85% for **1**-NCS and 70% for **2**-NCS).

The conversion of $[Fe^{II}(tmc)(OTf)](OTf)$ to **2** in the presence of $NBu_4BF_4$ can be conveniently monitored by UV/Vis/NIR spectroscopy with $PhI(OAc)_2$ as the oxidant, which unlike PhIO is a well-defined material and readily soluble in MeCN. Addition of only 1 equiv $PhI(OAc)_2$ to $[Fe^{II}(tmc)(OTf)](OTf)$ affords **1**-$NCCH_3$ quantitiatively in the absence or in the presence of $NBu_4BF_4$. Addition of a second equivalent $PhI(OAc)_2$ to the thus formed solution of **1**-

  

$NCCH_3$ does not effect any change in the absence of $NBu_4BF_4$, but converts **1**-$NCCH_3$ to **2** in the presence of $NBu_4BF_4$ (Figure 1). These results show that a minimum of 2 equiv $PhI(OAc)_2$ is required for the complete conversion of $[Fe^{II}(tmc)(OTf)](OTf)$ to **2**. The first equivalent generates **1**-$NCCH_3$, and the second transforms **1**-$NCCH_3$ to **2** in the presence of $NBu_4BF_4$.

What is the role of $NBu_4BF_4$? Experiments varying the amount of added $NBu_4BF_4$ show that a minimum of 0.2 equiv is required for the conversion of **1**-$NCCH_3$ to **2**. Furthermore, when excess $PhI(OAc)_2$ is present, **1**-$NCCH_3$ converts to **2** in a pseudo-first-order fashion over the course of minutes at room temperature (Figure 4); this rate of conversion increases

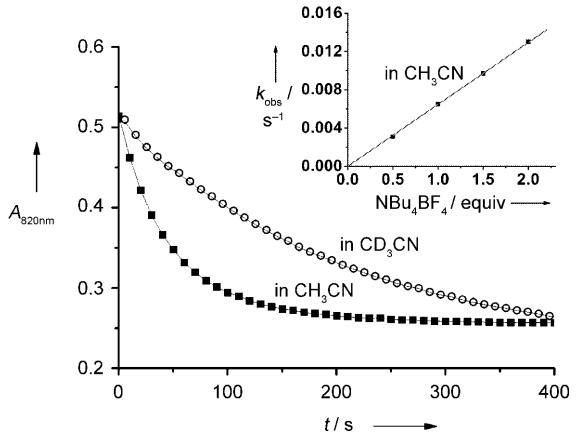


***Figure 4.*** The time traces for the formation of **2** from **1**-$NCCH_3$ under pseudo-first-order conditions (10 equiv $PhI(OAc)_2$ and 0.5 equiv $NBu_4BF_4$) in $CD_3CN$ ($k_{obs} = 0.0006\ s^{-1}$) and $CH_3CN$ ($k_{obs} = 0.003\ s^{-1}$) at 25 °C. Lines drawn through the experimental data represent the pseudo-first-order fits. The inset shows the dependence of the pseudo-first-order rate constant on the amount of $NBu_4BF_4$.

linearly with $NBu_4BF_4$ concentration (Figure 4 inset). We propose that the addition of $BF_4^-$ converts PhIO to $PhIOIPh(BF_4)_2$, which is known to be a more powerful oxidant than PhIO,[9] and this in situ generated oxidant reacts with **1**-$NCCH_3$ to generate **2**. In support of this proposal, **1**-$NCCH_3$ converts to **2** nearly quantitatively upon addition of 1 equiv isolated $PhIOIPh(BF_4)_2$.[9] Furthermore, when $^{18}O$-labeled **1**-$NCCH_3$ is treated with 1 equiv $PhI^{16}OIPh(BF_4)_2$, the resultant **2** is found to be $^{16}O$-labeled. Conversely, when $^{16}O$-labeled **1**-$NCCH_3$ is treated with $PhI^{18}OIPh(BF_4)_2$, **2** is found to be $^{18}O$-labeled. Thus the oxo atom of **2** derives not from the oxo atom of **1**-$NCCH_3$ but from the added oxidant. Based on these observations, a mechanism for the conversion of **1**-$NCCH_3$ to **2** is proposed in Scheme 1 that postulates formation of adduct **1a**, analogous to metal–oxo–oxidant adducts previously proposed to be more powerful oxidants than their parent metal–oxo species.[10] Formation of **1a** activates the Fe=O unit to oxidize the $CH_3CN$ solvent and form **2** either directly or via a transient dioxoiron(VI) species **1b**. In support, we observed a deuterium kinetic isotope effect of 5 for the conversion of **1**-$NCCH_3$ to **2**, when $CD_3CN$ was used as the solvent (Figure 4), so solvent C–H bond cleavage is rate-determining. Since both **1**-$NCCH_3$ and **2** have long half-lives in $CH_3CN$ ($t_{1/2} = 10$ and 7 h, respectively), a more powerful oxidant must be generated that is capable of cleaving the C–H bond of $CH_3CN$; we propose this oxidant to be either **1a** or **1b**. Thus, in the course of the conversion, the oxo group of **1**-$NCCH_3$ is effectively displaced by backside attack of $PhIOIPh(BF_4)_2$ to form its inverted isomer **2**.

Ruthenium analogues of the various species postulated in the mechanism shown in Scheme 1 have been reported by Che et al.[11] For example, $[Ru^{IV}(O)(tmc)(NCCH_3)]^{2+}$ is the ruthenium analogue of **1**-$NCCH_3$, with the oxo atom *anti* to all four N-methyl groups, while $[Ru^{IV}(O)(tmc)(NCO)]^+$ has a structure similar to that proposed for **2**, with the oxo atom *syn* to all four N-methyl groups. More importantly, $[Ru^{VI}(O)_2(tmc)]^{2+}$, the ruthenium analogue to the putative dioxoiron(VI) species **1b**, has also been characterized, lending credence to our dioxoiron(VI) hypothesis.

The most striking difference between **1**-$NCCH_3$ and **2** is in their reactivities. For example, **2** oxidizes $PPh_3$ and dihydroanthracene 35- and 170-fold faster, respectively, than **1**-$NCCH_3$ (Table S3). The greater reactivity of **2** is also reflected in the relative intermetal oxo-transfer abilities of the two isomers. Nam and co-workers[12] previously established an oxo-transfer hierarchy of **4** > **3** > **1**-$NCCH_3$ (**3** = $[Fe^{IV}(O)(N4Py)]^{2+}$); **4** = $[Fe^{IV}(O)(Bn\text{-}tpen)]^{2+}$; Bn-tpen = *N*-benzyl-*N*,*N*′,*N*′-tris(2-pyridylmethyl)-1,2-diaminoethane), with facile oxo transfer from **3** or **4** to $[Fe^{II}(tmc)(NCCH_3)]^{2+}$ to yield **1**-$NCCH_3$, but not from **1**-$NCCH_3$ to $[Fe^{II}(N4Py)(NCCH_3)]^{2+}$ and $[Fe^{II}(Bn\text{-}tpen)(NCCH_3)]^{2+}$. According to Nam's work,[12] this descending series reflects the progressive decrease in the $Fe^{IV}/Fe^{III}$ redox potential of the $Fe^{IV}$=O unit. In stark contrast to **1**-$NCCH_3$, **2** readily oxidizes $[Fe^{II}(N4Py)(NCCH_3)]^{2+}$ (Figure 5), $[Fe^{II}(Bn\text{-}tpen)(NCCH_3)]^{2+}$ (Figure S8), and $[Fe^{II}(tmc)(NCCH_3)]^{2+}$ (Figure S9) to corresponding oxo complexes **3**, **4**, and **1**-$NCCH_3$, respectively. Thus, **2** leapfrogs over the other three complexes, that is, **2** > **4** > **3** > **1**-$NCCH_3$, and is the most powerful oxidant in this series.

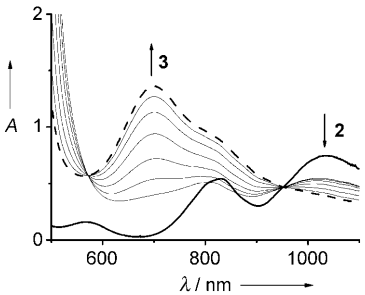


***Figure 5.*** Changes in the absorption spectrum associated with the reaction of a 4 mM solution of **2**, generated by addition of 2 equiv $PhI(OAc)_2$ and 0.2 equiv $NBu_4BF_4$ to $[Fe^{II}(tmc)(OTf)](OTf)$, with 1 equiv $[Fe^{II}(N4Py)(CH_3CN)]^{2+}$ in $CH_3CN$ at 25 °C.

The higher reactivity of **2** may arise from kinetic and/or thermodynamic factors.[7b] The axial iron site *syn* to the N-methyl groups may in fact be sterically less hindered, as suggested by the fact that anions bind only at this position in the structures of $[Fe^{II}(tmc)(X)]^+$ complexes,[6] so as to make **2** kinetically the more effective oxidant. On the other hand, the

  

intermetal oxo-transfer hierarchy established above, following Nam's arguments,[12] suggests that the higher oxidizing ability of **2** may reflect a higher $Fe^{IV}/Fe^{III}$ potential. DFT calculations on the two isomers (Figure S10, Tables S4 and S5) in fact support this thermodynamic argument, as **2** is calculated to be higher in energy than **1**-$NCCH_3$ by about 4 kcal mol$^{-1}$. A comparison of the two geometry-optimized structures suggests that the energy difference may arise from the 0.1 Å lengthening of the Fe–$NCCH_3$ bond in **2** accompanied by a 0.01 Å shortening of the Fe=O and Fe–$N_{tmc}$ bonds.[13] Establishing which factors determine the greater reactivity of **2** requires additional spectroscopic, electrochemical, and computational studies, which are in progress.

In summary, we reported herein spectroscopic evidence for the unexpected conversion of previously characterized **1**-$NCCH_3$ to its inverted isomer **2** by reaction with PhIOIPh-$(BF_4)_2$. Strikingly, the simple interchange of the positions of the axial oxo and $CH_3CN$ ligands between **1**-$NCCH_3$ and **2** significantly enhances the oxidative reactivity of the latter relative to the former, making these two complexes the first example of an isomer pair in which a particular face of a macrocyclic ligand affects reactivity so dramatically. Whatever the rationale, these results illustrate the subtle power of the coordination environment to tune the redox properties of the oxoiron(IV) unit.

Received: May 12, 2008
Revised: August 8, 2008
Published online: September 16, 2008

**Keywords:** bioinorganic chemistry · coordination modes · cyclam · high-valent compounds · nonheme iron complexes

[1] a) E. I. Solomon, T. C. Brunold, M. I. Davis, J. N. Kemsley, S.-K. Lee, N. Lehnert, F. Neese, A. J. Skulan, Y.-S. Yang, J. Zhou, *Chem. Rev.* **2000**, *100*, 235; b) M. Costas, M. P. Mehn, M. P. Jensen, L. Que, Jr., *Chem. Rev.* **2004**, *104*, 939; c) M. M. Abu-Omar, A. Loaiza, N. Hontzeas, *Chem. Rev.* **2005**, *105*, 2227.

[2] C. Krebs, D. Galonić Fujimori, C. T. Walsh, J. M. Bollinger, Jr., *Acc. Chem. Res.* **2007**, *40*, 484.

[3] a) X. Shan, L. Que, Jr., *J. Inorg. Biochem.* **2006**, *100*, 421; b) L. Que, Jr., *Acc. Chem. Res.* **2007**, *40*, 493.

[4] J.-U. Rohde, J. H. In, M. H. Lim, W. W. Brennessel, M. R. Bukowski, A. Stubna, E. Münck, W. Nam, L. Que, Jr., *Science* **2003**, *299*, 1037.

[5] B. Bosnich, C. K. Poon, M. L. Tobe, *Inorg. Chem.* **1965**, *4*, 1102.

[6] a) C. V. Sastri, M. J. Park, T. Ohta, T. A. Jackson, A. Stubna, M. S. Seo, J. Lee, J. Kim, T. Kitagawa, E. Münck, L. Que, Jr., W. Nam, *J. Am. Chem. Soc.* **2005**, *127*, 12494; b) A. T. Fiedler, H. L. Halfen, J. A. Halfen, T. C. Brunold, *J. Am. Chem. Soc.* **2005**, *127*, 1675.

[7] a) A. Decker, J.-U. Rohde, L. Que, Jr., E. I. Solomon, *J. Am. Chem. Soc.* **2004**, *126*, 5378; b) A. Decker, J.-U. Rohde, E. J. Klinker, S. D. Wong, L. Que, Jr., E. I. Solomon, *J. Am. Chem. Soc.* **2007**, *129*, 15983.

[8] a) W. J. Geary, *Coord. Chem. Rev.* **1971**, *7*, 81; b) L. Casella, J. A. Ibers, *Inorg. Chem.* **1981**, *20*, 2438.

[9] V. V. Zhdankin, R. Tykwinski, B. Berglund, M. Mullikin, R. Caple, N. S. Zefirov, A. S. Koz'min, *J. Org. Chem.* **1989**, *54*, 2609.

[10] a) N. Y. Oh, M. S. Seo, M. H. Lim, M. B. Consugar, M. J. Park, J.-U. Rohde, J. Han, K. M. Kim, J. Kim, L. Que, Jr., W. Nam, *Chem. Commun.* **2005**, 5644; b) Y. Suh, M. S. Seo, K. M. Kim, Y. S. Kim, H. G. Jang, T. Tosha, T. Kitagawa, J. Kim, W. Nam, *J. Inorg. Biochem.* **2006**, *100*, 627; c) S. H. Wang, B. S. Mandimutsira, R. Todd, B. Ramdhanie, J. P. Fox, D. P. Goldberg, *J. Am. Chem. Soc.* **2004**, *126*, 18; d) X. Shan, L. Que, Jr., *Chem. Commun.* **2008**, 2209.

[11] a) C. M. Che, K. Y. Wong, T. C. W. Mak, *J. Chem. Soc. Chem. Commun.* **1985**, 546; b) C. M. Che, T. F. Lai, K. Y. Wong, *Inorg. Chem.* **1987**, *26*, 2289.

[12] C. V. Sastri, K. Oh, Y. J. Lee, M. S. Seo, W. Shin, W. Nam, *Angew. Chem.* **2006**, *118*, 4096; *Angew. Chem. Int. Ed.* **2006**, *45*, 3992.

[13] The DFT calculated differences in Fe=O and Fe–$N_{tmc}$ bond lengths for **1**-$NCCH_3$ and **2** are within the error of EXAFS analysis.

  